Electronic Supplementary Material (ESI) for Journal of Materials Chemistry B.

Near-infrared Irradiation Controlled Thermo-Switchable Polymeric Photosensitizer against β-Amyloid Fibrillation

Li Chen,[a] Zhe Zhou,[b] Yuexing Zhang,[a] Jie Pan,[a] Kai Wang,*[a] and Hang-Xing Wang*[a]

[a] L. Chen, Dr. Yue-Xing Zhang, Dr. J. Pan, Prof. K. Wang, and Prof. H. X. Wang,
College of Chemistry and Chemical Engineering, Hubei University, Wuhan, 430062, China
E-mail: wanghx0917@163.com, kaiwang@hubu.edu.cn

[b] Z. Zhou
Department of Neurology, the First Hospital of Lanzhou University, Lanzhou University, Lanzhou, Gansu, 730000, China.

Keywords: hydroxypropyl cellulose, the lower critical solution temperature, polymeric photosensitizer, inhibiting Aβ aggregation, dissociating Aβ aggregates

Table of Contents

1. Pioneering works

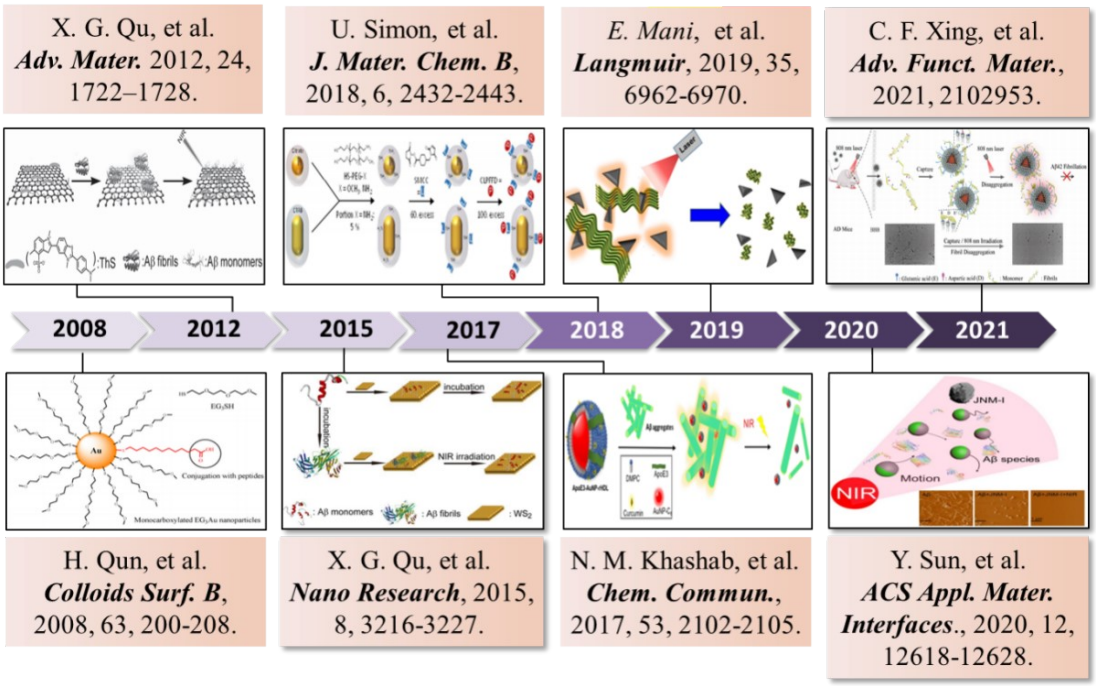

Scheme S1. Timeline providing examples of photothermal materials for modulating Aβ assembly by PTT. [1-8]

2. Experimental Procedures

2.1. Apparatus and Chemicals

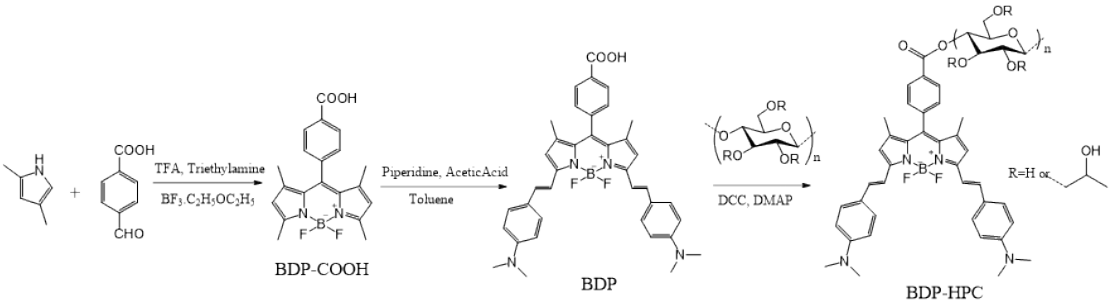

Scheme S2. The synthetic route of BDP-HPC.

UV-vis absorption spectrum and fluorescence Spectroscopy were recorded on UV-vis spectrophotometer (TU-1901, Beijing) and spectrofluorometer (FL-6000, Japan), respectively. Dynamic Light Scattering (DLS) and Transmission Electron Microscope (TEM) images were obtained from Zetasizer Nano ZS90 Nanometer particle size potentiometer (Malvern, Britain) and JEM-200 transmission electron microscope (JEOL, Japan). Circular dichroism (CD) spectra were measured on a Chirascan Series Spectrometer (Applied Photophysics, Britain).

Hydroxypropyl cellulose (HPC, average Mw: ~80,000, average Mn: ~10,000), 2,4-Dimethyplyrrole, 4-Formylbenzoic acid, trifluoroacetic acid (TFA), Tetrachioro pbenzoquinone, boron(tri) fluoride etherate, 4-Dimethylaminobenzaldehyde, Acetic Acid, piperidine, N, N'-Dicyclohexylcarbodiimide (DCC), 4-(Dimethylamino)pyridine (DMAP). Thioflavin T (ThT) was purchased from Sigma. 1,1,1,3,3,3-hexafluoro-2-propanol (HFIP) and 3-(4,5-dimethyl-2-thiazolyl)-2,5-diphenyl-2H-tetrazolium bromide (MTT) were obtained from Aladdin Industrial Cooperation (Shanghai, China). Beta-Amyloid (1-42) ($A\beta_{42}$), Human was synthesized in Suzhou Qiangyao Biotechnology Co., Ltd. (China Peptides Co., Ltd.). These chemical products were used without further purification process. N, N-Dimethylformamide (DMF), methylbenzene, and triethylamine used in the experiment were refluxed with calcium hydride and then distilled under reduced pressure. Millipore ultrapure water with a certain resistivity >18.25 MΩ·cm was used throughout the experiment. The working solution was using a 50 μM phosphate buffer solution (PBS, pH=7.4).

2.2 Synthesis of BDP-COOH

A solution of 2,4-dimethyplyrrole (0.52 g, 5.31 mmoL) and 4-formylbenzoic acid (0.40 g, 2.66 mmoL) in dichloromethane (50 mL), then TFA (100 μL) was added. The mixture was stirred for 6 hours at room temperature and added Tetrachioro-p-benzoquinone (1.30 g, 5.02 mmoL) for an additional 1 h. Finally, triethylamine (8 mL) and boron tri-fluoride etherate (8 mL) was added to a mixture, keep stirring for 30 mins at room temperature. Then the solvent was removed and the mixture was extracted with dichloromethane three times, the combined organic layer was dried with anhydrous Na_2SO_4 and concentrated. Finally, the residue was purified by column chromatography (silica gel, CH_2Cl_2/methanol=120:1) to afford BDP-COOH as a red solid (0.56 g, yielding 65%). ^{1}H NMR (600 MHz, $CDCl_3$): δ 8.21-8.25 (d, 2H, Ph-H), 7.43-7.47 (d, 2H, Ph-H), 6.00 (s, 2H, CH_2), 2.56 (s, 6H, CH_3), 1.37 (s, 6H, CH_3).

2.3 Synthesis of BDP

BDP-COOH (20 mg, 0.05 mmoL) 4-Dimethylaminobenzaldehyde (24.3 mg, 0.16 mmoL), acetic acid (0.23 g, 3.80 mmoL), and piperidine (0.17 g, 2.17 mmoL) were dissolved in 25 mL methylbenzene, the mixture was stirred for 6 hours at 130 ^{o}C. Then the solvent was removed and the mixture was extracted with dichloromethane several times, the combined organic layer was dried with anhydrous Na_2SO_4 and concentrated. Finally, the residue was purified by column chromatography (silica gel, CH_2Cl_2/methanol=90:1) to afford BDP as a red solid (12 mg, yielding 23 %). ^{1}H NMR (500 MHz, $CDCl_3$): δ 7.35-7.75 (d, 8H, Ph-H), 6.65-6.75 (d, 4H, Ph-H), 5.30 (s, 2H, CH_2), 2.90-3.05 (d, 12H, CH_3), 1.36-1.41 (s, 6H, CH_3).

2.4. Synthesis of BDP-HPC

HPC (0.38 g, 0.05 mmoL) was dissolved in DMF (5 mL) was added, and the mixture was purged with nitrogen for 6 h. Then BDP (5.20 mg, 0.01 mmoL), DCC (24 mg, 0.12 mmoL), and DMAP (24 mg, 0.19 mmoL) were added. The mixture was stirred at room temperature for 2 days under nitrogen and the reactant was precipitated in cold ether

(0.2 L) and repeated several times. The resultant was dialyzed against deionized water using a cellulose membrane to remove unreacted impurities. The final products were lyophilized and stored in a refrigerator at -20 ^{o}C.

2.5 Preparation of $A\beta_{42}$ monomers, oligomers, and fibrils

The $A\beta_{42}$ peptide power was dissolved in 1,1,1,3,3,3-hexafluoroisopropanol (HFIP) at a concentration of 1 mg/mL. To destroy the pre-existing $A\beta_{42}$ aggregates, the solution was in quiescence for 20 min and then sonicated in an ice bath for 5 min. Subsequently, the resulting solution was centrifuged for 30 min at 1200 r/min to remove any pre aggregates. The supernatant was absorbed with a pipettor, then freeze-dried and stored in dark at -30 ^{o}C before use. To prepare oligomers and fibrils, the peptide was then resuspended in phosphate buffer saline (containing 0.02 % sodium azide, pH 7.4) at a final concentration of 50 μM and then incubated at 37 °C for the different times with continuous shaking (400 rpm).

2.6 Characterization of the binding affinity and selectivity toward $A\beta_{42}$

The $A\beta_{42}$ fibrils (50 μM, 250 μL, pre-incubated for 24 hours) were treated with BDP-HPC (5 mg/mL, 50 μL) and incubated for 2 hours, evenly spread on a glass slide, and fluorescent images were recorded. To further verify the binding affinity of BDP-HPC to $A\beta_{42}$, BDP-HPC was added to ThT (25 μM, 50 μL) -labeled $A\beta_{42}$ fibrils, and then incubated for 2 hours, and fluorescence images were recorded. $A\beta_{42}$ fibrils were used alone, and ThT-labeled $A\beta_{42}$ fibrils were used as a control group.

2.7 Cytotoxicity Assay

PC12 cells were cultured in Dulbecco's modified Eagle's medium (DMEM) containing 10 % fetal bovine serum at 37 ^{o}C. For in vitro therapeutic efficacy tests, PC12 cells were seeded on 96-well plates with DMEM culture media. After incubation for 24 h, the cells were incubated with BDP-HPC (0-5.0 mg/mL) for another 24 h, the cell viability was evaluated with the MTT method. To assess the effect of NPs on the cell toxicity of $A\beta_{42}$, $A\beta_{42}$ aggregates (20 μM) with BDP-HPC for an equilibration time

of 2 h were irradiated upon 680 nm laser for 0.5, 1.0, and 2.0 h (1 W·cm^{-2}). The $A\beta_{42}$ aggregates containing BDP-HPC were kept at 37 ^{o}C for 3 h after laser irradiation. Then PC12 cells were treated with $A\beta_{42}$ and BDP-HPC complex for an additional 48 h and the cell viability was examined.

2.8 Singlet oxygen generation efficiency

1,3-Diphenylisobenzofuran (DPBF) was used as selective singlet oxygen ($^1O_2$) acceptor, which was bleached upon reaction with $^1O_2$. The compounds with DPBF in DMF (50 mM) were prepared in the dark.[9] Each sample container was covered with aluminum foil with a yellow filter (with a cut-off wavelength < 500 nm) on one side. The samples were then exposed to light (50 watts) through the filter. The photodegradation rate of DPBF was calculated by recording the absorption intensity at 418 nm. The linear slope reflected the $^1O_2$ production rate of different porphyrin compounds. The bigger slope indicated the higher efficiency of $^1O_2$ generation.

2.9 Photothermal Performance of BDP-HPC

The aqueous solution of BDP-HPC (3.0 mL) in a quartz cell with different concentrations (0, 2.5, 5, 10 mg/mL) was irradiated by a 680 nm laser for 600 s at different power density values (0.5, 1.0, 1.5, 2.0 W·cm^{-2}). For comparison, pure water and HPC were used as a control sample. The temperature and the thermal images of solutions were monitored and collected every 60 s during irradiation by an IR-thermal camera.

2.10 Photothermal conversion efficiency of BDP-HPC

The photothermal conversion efficiency (η) of the BDP-HPC was calculated according to the reported method.[10-12] Under continuous laser irradiation, the temperature of the BDP-HPC aqueous solution was recorded, until the solution had reached a steady-state temperature at 1200 s. The photothermal conversion efficiency (η) was calculated according to Equation (1):

$$\eta = \frac{hA(T_{Max} - T_{Surr}) - Q_{Dis}}{I(1 - 10^{-A680})} \quad (1)$$

Where *h* represented the heat transfer coefficient. A was the surface area of the quartz sample cell. T_{Max} and T_{Surr} were the maximum steady-state temperature (55.5 ^{o}C) and the surrounding temperature of the environment (26.2 ^{o}C), respectively. Q_{Dis} is the heat dissipation from the light absorbed by the solvent and the quartz sample cell. *I* was the incident laser power (1 W/cm^2), and *A680* was the absorbance intensity of the sample at 680 nm (1.5). The value of *hA* was derived from Equation (2):

$$\tau_s = \frac{m_D c_D}{hA} \quad (2)$$

Where τ was the time constant for heat transfer of the system which was determined to be τ= 374.6 from Figure 3e. m_D and c_D were the mass (3.0 g) and heat capacity (4.2 J/g) of the deionized water utilized to dissolve the BDP-HPC, respectively. The *hA* was determined as 0.0336 W. Q_{Dis} represented the heat dissipation from the light absorbed by the water and the quartz sample cell, and Q_{Dis} was calculated according to Equation (3):

$$Q_{Dis} = \frac{c_D m_D (T_{Max(water)} - T_{Surr})}{\tau_{s(water)}} \quad (3)$$

Where $T_{max(water)}$= 35.9 ℃, $T_{max(surr)}$= 23.6 ℃, $\tau_{(water)}$= 679.9, so Q_{dis} was calculated to be 0.228 W. According to the obtained data and Equation (1), the photothermal conversion efficiency of the 0.0336 W was determined to be 78.1 %.

2.11 SDS-PAGE test

SDS-PAGE method was used to determine the ability of BDP-HPC to dissociate $A\beta_{42}$ fibrils. $A\beta_{42}$ species including monomers (20 μM, 20 μL), oligomers (20 μM, 20 μL), fibrils (10 μM, 20 μL), and fibrils & BDP-HPC after irradiation by a NIR laser for 120 mins with an irradiation intensity of 1 W/cm^2 (fibrils: 20 μM, 20 μL; BDP-HPC: 5 mg/mL, 10 μL) mixture were separated and denatured by boiling for 5 min in loading buffer (Coolaber 3 × protein loading buffer with DTT, 20 μL). These four samples were separated by size in the moiety of porous 12.5 % polyacrylamide gel (1D SDS-PAGE),

in an electric field using a Mini-PRO4 electrophoresis system from WIX. The electrophoresis was run under constant voltage (120 V, 80 min). The gels were stained using silver stain (Beyotime) for 2 h, followed by destaining overnight in deionized water.

2.12 In vivo imaging

The wild-type mouse was intravenously injected with BDP-HPC (80 μg/mL) after shaving, the mice were kept in the imaging stage under anesthesia with 2 % isoflurane gas in an oxygen flow (1.5 L/min) during the imaging process. Fluorescence signals from the brain were recorded at different time points (0-6 h) after intravenous injection of BDP-HPC (λ_{ex} = 600 nm, λ_{em} = 750 nm) by using IVIS Spectrum PerkinElmer the in vivo fluorescence imaging system, and optical images were acquired using an exposure time of 2 s. Imaging data were analyzed by Living Image Software. All of the animal experiments were carried out in accordance with the relevant laws and guidelines issued by the Ethical Committee of Hubei University and were in agreement with the guidelines of the Institutional Animal Care and Use Committee.

3. Figures

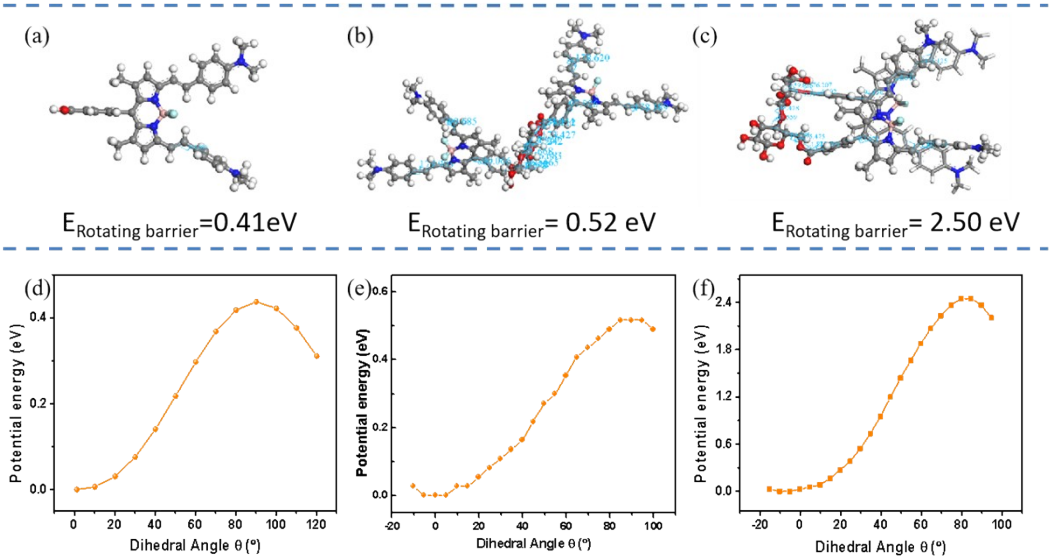

Figure S1. Rigid scan results by changing dihedral angle and calculating the energy. Calculated with B3LYP functional and 6-31+g (d, p) basis set in water solvent using IEFPCM solvent model using Gaussian 16 software.

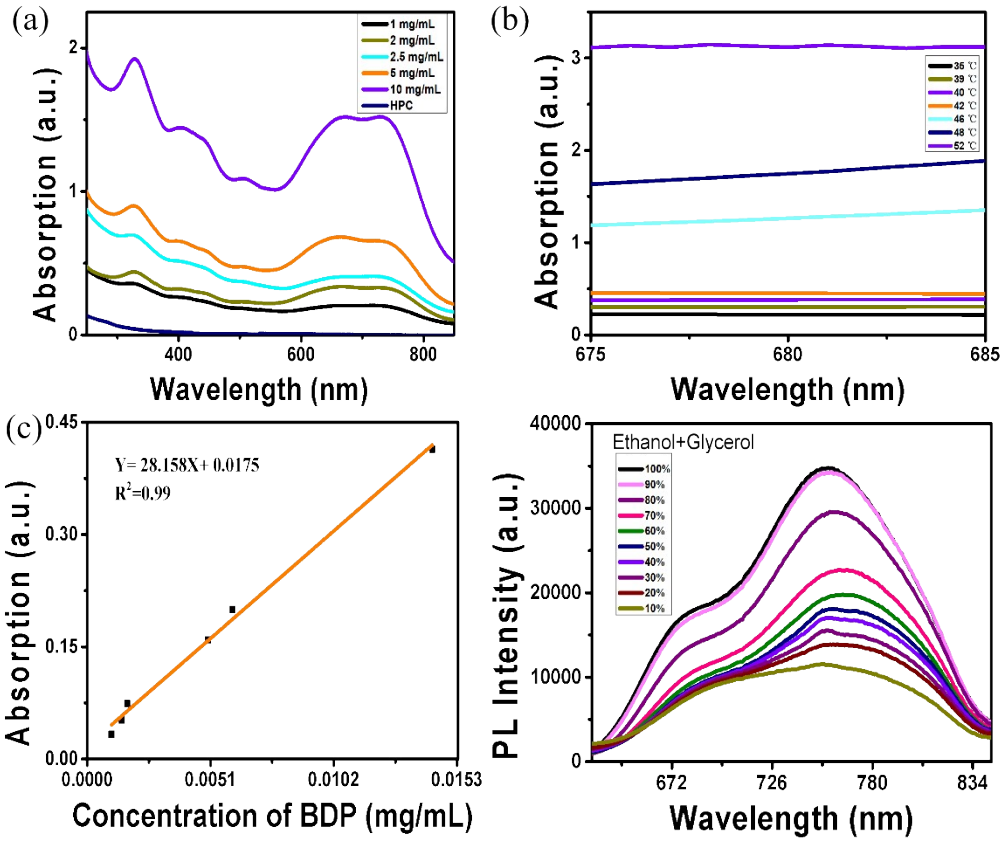

Figure S2. (a) UV-vis absorption spectra of different concentrations of BDP-HPC in water; (b) A linear regression curve obtained by plotting the absorbance (at 680 nm) of BDP at different concentrations; (c) Changes in UV-vis absorption of BDP-HPC in water at different temperature. (d) Fluorescence emission spectra of BDP in different ratios of ethanol and glycerol solutions.

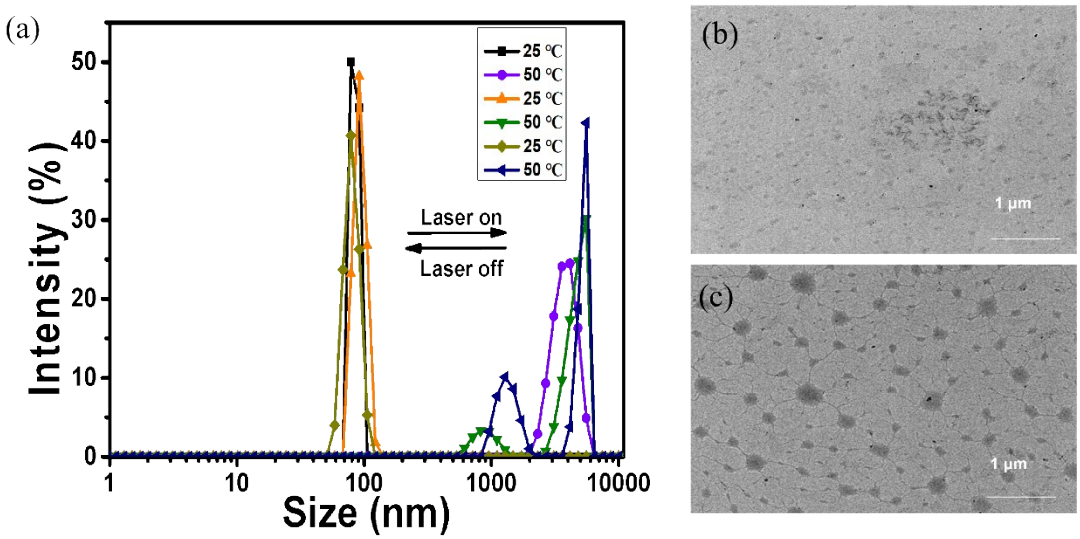

Figure S3. (a) DLS image of particle size changing of BDP-HPC for five alternate on/off laser irradiation cycles (680 nm, 5 min); TEM image of BDP-HPC samples prepared at (b) room temperature and (c) under irradiation of 680 nm laser for 5 min. (BDP-HPC: 5 mg/mL).

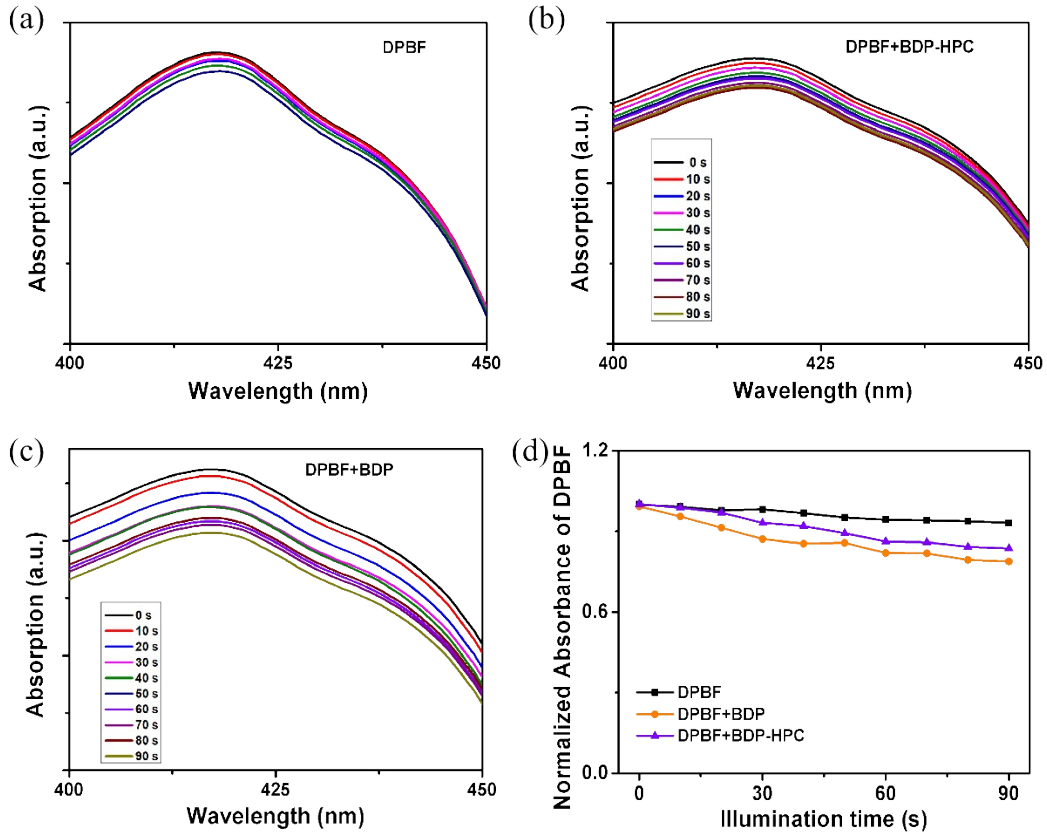

Figure S4. (a) UV-vis absorption spectrum of different time periods after DPBF was irradiated at 689 nm (50 Mw/cm^2) to generate ROS (a) blank sample; (b) BDP-HPC; (c) BDP; (d) Singlet oxygen generation of BDP and BDP-HPC (50 mM). The change of absorption of DPBF at 418 nm (A/A_0) upon the irradiation time. The spectrum was recorded in DMF.

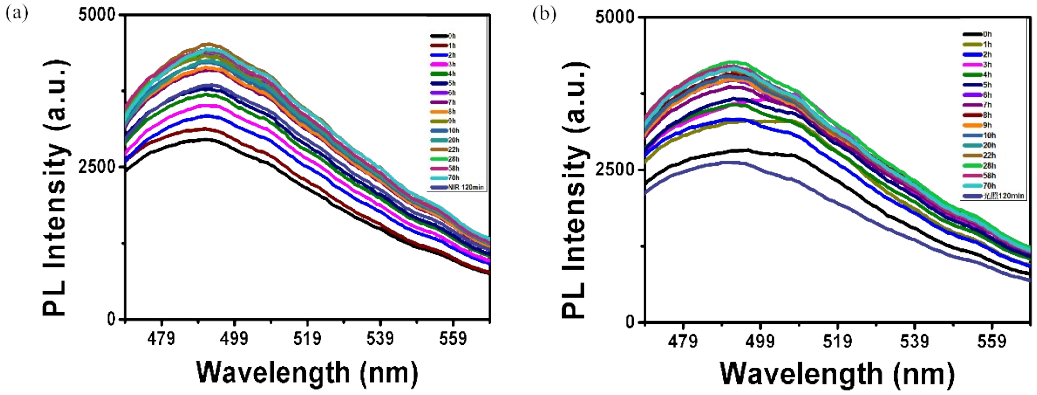

Figure S5. ThT fluorescence assay of (a) $A\beta_{42}$ fibrils and (b) $A\beta_{42}$ fibrils in the presence of BDP-HPC under 680 nm irradiation for 2 h (1 W/cm^2). ($A\beta_{42}$: 50 μM, BDP-HPC:5 mg/mL, ThT: 10 μM, λ_{ex}= 437 nm, λ_{em}= 455 nm).

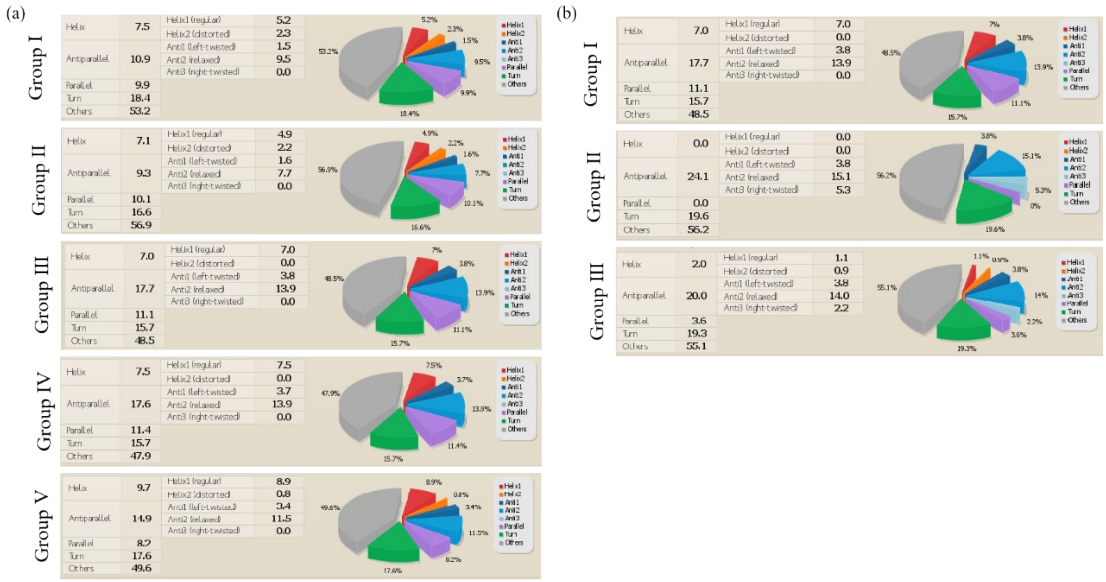

Figure S6. (a) Photothermal inhibition of $A\beta_{42}$ aggregation was quantified using the BeStSel Web Server. Group Ⅰ: $A\beta_{42}$ monomers; Group Ⅱ: $A\beta_{42}$+BDP-HPC; Group Ⅲ: $A\beta_{42}$ fibrils; Group Ⅳ: $A\beta_{42}$+BDP-HPC (in dark); Group Ⅴ: $A\beta_{42}$+BDP-HPC (with laser on/off); (b) quantitative analysis of the structural characterization of photothermal dissociated $A\beta_{42}$ fibers using the BeStSel Web Server. Group Ⅰ: $A\beta_{42}$ fibrils; Group Ⅱ: $A\beta_{42}$+BDP-HPC (NIR 1 h); Group Ⅲ: $A\beta_{42}$+BDP-HPC (NIR 2 h).

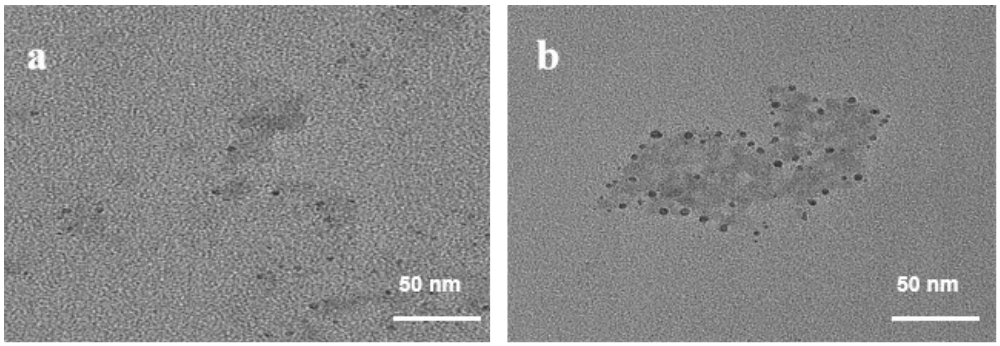

Figure S7. TEM images of $A\beta_{42}$ fibrils in the presence of BDP-HPC under 680 nm illumination for 2 h. Scale bars: 50 nm. ($A\beta_{42}$: 50 μM, BDP-HPC: 5 mg/mL).

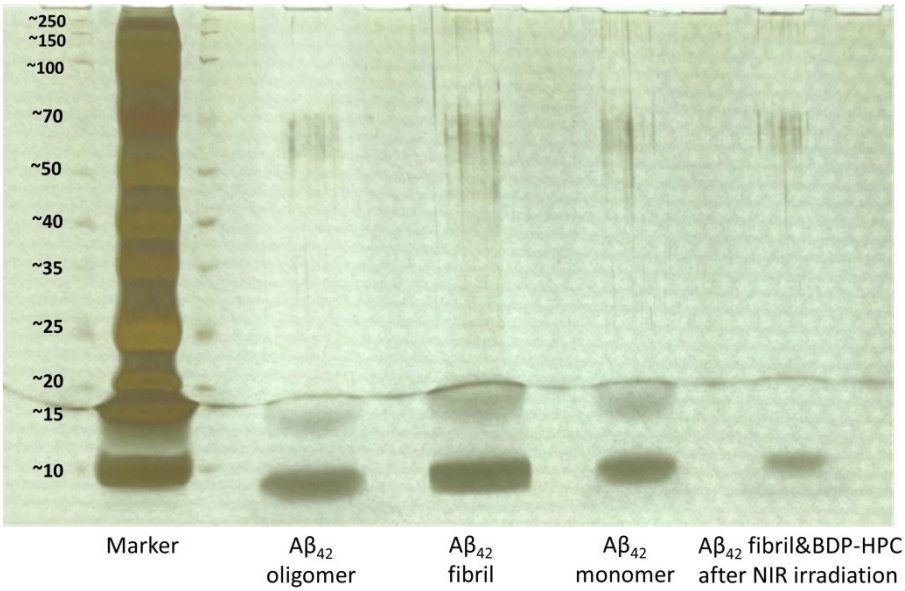

Figure S8. Protein bands from the SDS-PAGE gel of $A\beta_{42}$ species including $A\beta_{42}$ oligomer (lane 2), $A\beta_{42}$ fibril (lane 3), $A\beta_{42}$ monomer (lane 4), and $A\beta_{42}$ fibril & BDP-HPC mixture (lane 5) after irradiation by a NIR laser for 120 mins with an irradiation intensity of 1 W/cm^2.

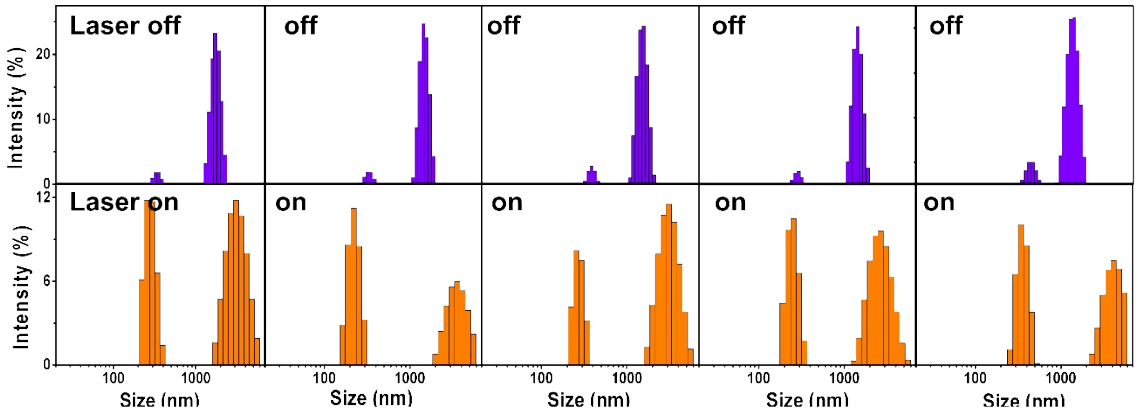

Figure S9. DLS image of particle size changing of BDP-HPC and $A\beta_{42}$ for five alternate on/off laser irradiation cycles ($A\beta_{42}$: 30 μM, BDP-HPC: 5 mg/mL, 680 nm, 1 W/cm^2).

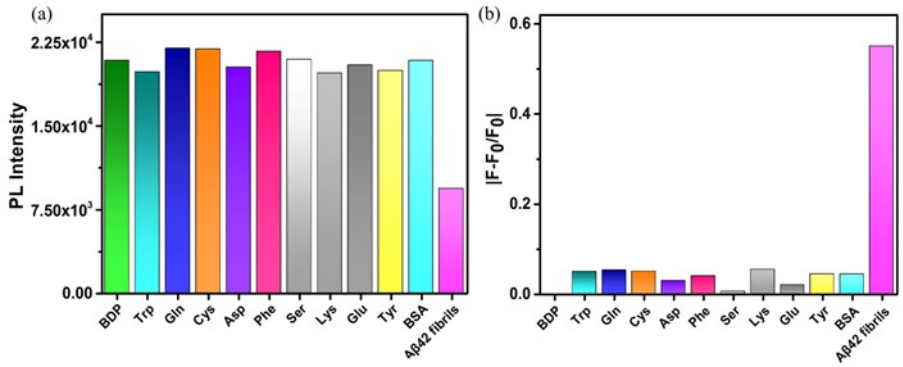

Figure S10. Anti-interference experiments of amino acids and proteins on BDP fluorescence. (a) The Fluorescence emission spectroscopy of BDP treated with different amino acids (50 μM), BAS protein (50 μM), and $A\beta_{42}$ fibrils (50 μM). (b) The change of fluorescent intensity of BDP towards amino acids, BAS protein, and Aβ42 fibrils.

Noted: We selected several small molecular amino acids (such as tryptophan; glutamine; cysteine; aspartic acid; phenylalanine; serine; lysine; glutamic acid; tyrosine) and bovine serum albumin (BAS) as control groups to explore the specificity of BDP-HPC to $A\beta_{42}$ fibrils. As shown in Figure S9, the fluorescence of BDP decreased only after binding to $A\beta_{42}$ fibrils, whereas the fluorescence change of the control experimental samples could be negligible after binding to BDP suggesting that these amino acids and BAS have no significant effect on the specific binding of BDP to $A\beta_{42}$ protein.

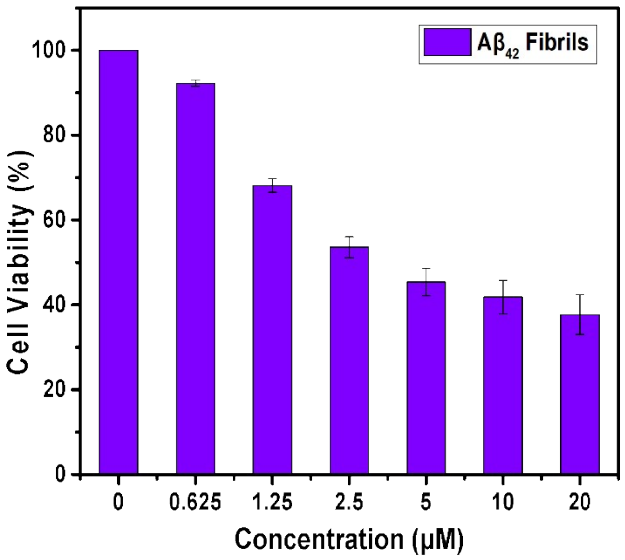

Figure S11. Viability of PC12 cell treated with various concentrations of $A\beta_{42}$ fibrils (0-20 μM).

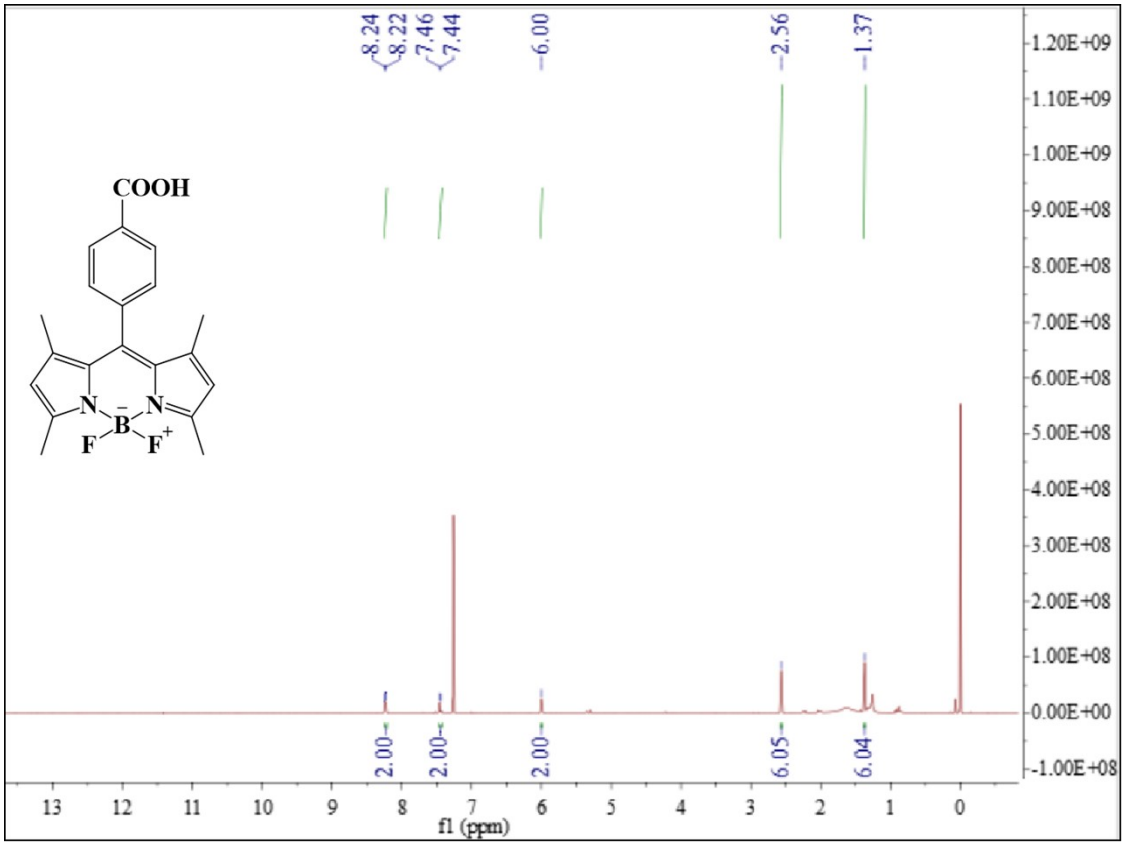

Figure S12. ^{1}H-NMR analysis of BDP-COOH in $CDCl_3$-*d.*

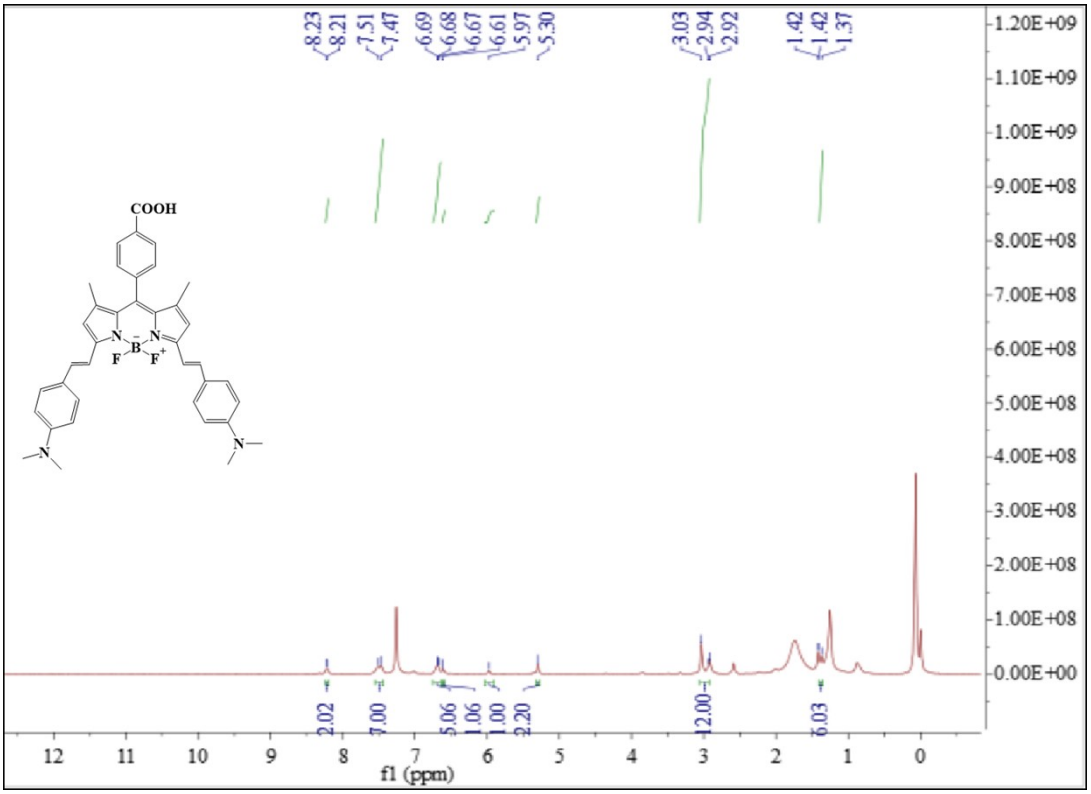

Figure S13. ^{1}H-NMR analysis of BDP in $CDCl_3$-*d*.

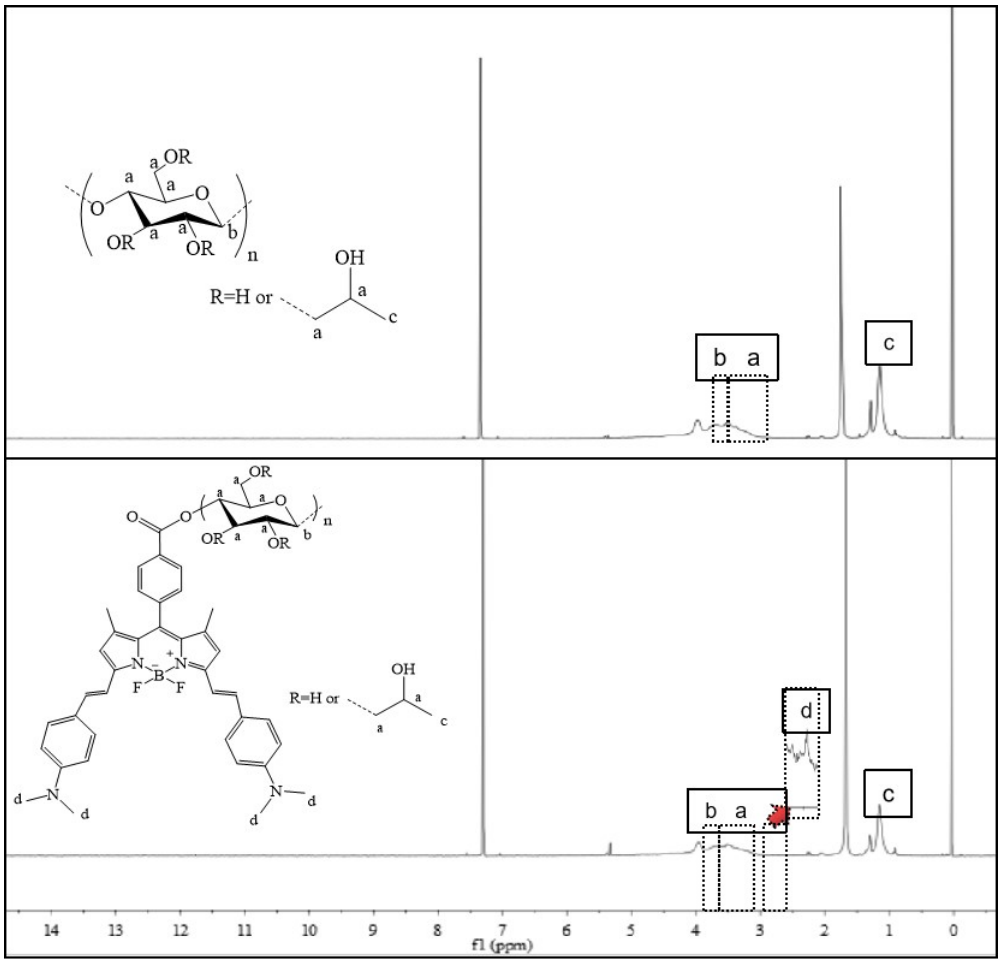

Figure S14. ^{1}H-NMR analysis of native HPC and BDP-HPC in $CDCl_3$-*d.*

References

1. C. R. Triulzi, Q. Dai, J. H. Zou, M. R. Leblanc, Q. Gu, J. Orbulescu, and Q. Huo, Photothermal Ablation of Amyloid Aggregates by Gold Nanoparticles, *Colloids Surf. B*., 2008, **63**, 200-208.
2. M. Li, X. J. Yang, J. S. Ren, and K. G. Qu, Using Graphene Oxide High Near-Infrared Absorbance for Photothermal Treatment of Alzheimer's Disease, *Adv. Mater.,* 2012, **24**, 1722-1728.
3. M. Li, A. D. Zhao, K. Dong, W. Li, J. S. Ren, and X. G. Qu, Chemically Exfoliated WS2 nanosheets Can Efficiently Inhibit Amyloid β-Peptide Aggregation and Use for Photothermal Treatment of Alzheimer's Disease, *Nano Res.,* 2015, **8**, 3216-3227.
4. A. T. Martins, S. Alsaiari, K. Julfakyan, Z. Nie, and N. M. Khasha, Self-Assembled Lipoprotein Based Gold Nanoparticles for Detection and Photothermal Disaggregation of β-Amyloid Aggregates, *Chem. Commun*., 2017, **53**, 2102-2105.
5. J. Ruff, N. Hassan, M. F. Zavala, J. Steitz, E. Araya, J. M. Kogan, and U. Simona, CLPFFD-PEG Functionalized NIR-absorbing Hollow Gold Nanospheres and Gold Nanorods Inhibit ß-Amyloid Aggregation, *J. Mater. Chem. B*, 2018, 6, 2432-2443.
6. S. Sudhakar and E. Mani, Rapid Dissolution of Amyloid # Fibrils by Silver Nanoplates, *Langmuir*, 2019, **35**, 6962-6970.
7. W. Liu, W. J. Wang, X. Y. Dong, and Y. Sun, Near-Infrared Light-Powered Janus Nanomotor Significantly Facilitates Inhibition of Amyloid-β Fibrillogenesis, *ACS Appl. Mater. Interfaces*, 2020, **12**, 12618-12628.
8. H. Geng, Y. C. Pan, R. Zhang, D. Gao, Z. J. Wang, B. Y. Li, D. S. Guo, and C. F. Xing, Binding to Amyloid-β Protein by Photothermal Blood-Brain Barrier-Penetrating Nanoparticles for Inhibition and Disaggregation of Fibrillation, *Adv. Funct. Mater.*, 2021, **2102953**.
9. Q. Y. Tang, W. Y. Xiao, C. H. Huang, W. L. Si, J. J. Shao, W. Huang, P. Chen, Q. Zhang, and X. C. Dong, pH-Triggered and Enhanced Simultaneous Photodynamic and Photothermal Therapy Guided by Photoacoustic and Photothermal Imaging, *Chem. Mater.,* 2017, **29**, 5216−5224.

10. F. Wu, L. Chen, L. Yue, K. Wang, K. Cheng, J. Chen, X. Luo, and T. Zhang, Small-Molecule Porphyrin-Based Organic Nanoparticles with Remarkable Photothermal Conversion Efficiency for in Vivo Photoacoustic Imaging and Photothermal Therapy, *ACS Appl. Mater. Interfaces,* 2019, **11**, 21408-21416.
11. Y. J. Liu, P. Bhattarai, Z. F. Dai, and X. Y. Chen, Photothermal Therapy and Photoacoustic Imaging via Nanotheranostics in Fighting Cancer, *Chem. Soc. Rev.*, 2019, **48**, 2053-2108.
12. Y. Cai, P. P. Liang, Q. Y. Tang, X. Y. Yang, W. L. Si, W. Huang, Q. Zhang, and X. C. Dong, Diketopyrrolopyrrole-Triphenylamine Organic Nanoparticles as Multifunctional Reagents for Photoacoustic Imaging-Guided Photodynamic/Photothermal Synergistic Tumor Therapy, *ACS Nano*, 2017, **11**, 1054-1063.